Optical Rectification*

M. BASS,† P. A. FRANKEN, AND J. F. WARD‡
The Harrison M. Randall Laboratory of Physics, University of Michigan, Ann Arbor, Michigan
(Received 23 November 1964)

Optical rectification, which is the production of a steady polarization in certain crystals by the action of an intense optical electric field, was first observed in crystals of KH_2PO_4 upon transmission of ruby-laser radiation. The present paper describes measurements for several crystals, which have been accomplished with an improved version of the original technique. Values for the appropriate macroscopic coefficients are: $(X_{xxy}^0+X_{xyx}^0)$ $(KH_2PO_4)=5\times10^{-8}$ esu; $(X_{xxy}^0+X_{xyx}^0)$ $(KD_2PO_4)=10.5\times10^{-8}$ esu; X_{zxx}^0 (CdS) $=45\times10^{-8}$ esu; X_{zzz}^0 (CdS) $=35\times10^{-8}$ esu; X_{zxx}^0 $[Cd(S_{0.75}+Se_{0.25})]=145\times10^{-8}$ esu; and $(X_{xxy}^0+X_{xyx}^0)$ (ZnTe) $=365\times10^{-8}$ esu. These absolute values are considered reliable only to within a factor 3, owing largely to uncertainty in determining the ruby-laser beam intensity. The relative values, however, are considered to be reliable within 50%. These results are compared with theoretical predictions and found to be consistent with the currently accepted quantum-mechanical theory of nonlinear optical phenomena. In particular, the intimate connection between the linear electro-optic effect (Pockel's effect) and optical rectification now appears to be firmly established. The theory can also be used, with some severe approximations, to yield crude predictions of the relative values obtained in the present experiments.

I. INTRODUCTION

OPTICAL rectification refers to the development of a steady polarization that accompanies the passage of an intense beam of light through certain crystals. This effect is related to several nonlinear optical phenomena which have received recent attention,[1] and which have offered some novel insight into the structure of optical mechanisms in a variety of media.

The simplest nonlinear dependence of the optical polarization p on an applied optical electric field E is $p\propto E^2$. If E has a $\sin\omega t$ time dependence, then this nonlinear relation predicts $p\propto\sin^2\omega t=\frac{1}{2}(1-\cos2\omega t)$. That part of the polarization with a $\cos2\omega t$ dependence is responsible for the radiation of second harmonic from certain crystals, whereas the unit term describes the steady polarization referred to as optical rectification. It is important to note that the amplitudes of these two contributions are not, in general, as simply related as is indicated by this approach. This expression is in a simplified scalar form and also is appropriate only to those circumstances in which the frequency ω is very small compared to any relevant natural frequencies or resonances in the crystal (the classical limit). More general circumstances require a formalism that takes cognizance of both the resonance phenomena and the restrictions imposed by the crystal symmetry.

An intimate relationship exists between optical rectification and the linear electro-optic effect that obtains at all frequencies of excitation. This relationship was first recognized by Armstrong *et al.*,[2] and is reviewed in Sec. III. The linear electro-optic effect (Pockel's effect) refers to the modification of the refractive indices of certain crystals by a low-frequency (or dc) electric field, and is a nonlinear optical process of the same order as optical rectification. Both of these processes are most conveniently described by tensors $\mathbf{X}$ which relate the electric fields E to the ensuing nonlinear polarizations p:

$$\text{(optical rectification)}\qquad p_i^0=X_{ijk}^0E_j^\omega E_k^\omega, \quad \text{(I.1a)}$$

$$\text{(linear electro-optic effect)}\qquad p_j^\omega=X_{jik}^\omega E_i^0E_k^\omega. \quad \text{(I.1b)}$$

In these equations the superscripts serve to indicate relevant frequencies; the X_{ijk}^0 and X_{jik}^ω are elements of third-rank tensors characteristic of the particular crystal; the quantities E_j^0, E_k^ω, p_i^ω, etc., refer to the *amplitudes* of the fields and polarizations; and the convention of summation over repeated indices is adopted.

Since $E_j^\omega E_k^\omega$ is physically indistinguishable from $E_k^\omega E_j^\omega$, experiments on optical rectification can only reveal the magnitude of pairs of coefficients: $(X_{ijk}^0+X_{ikj}^0)$. Furthermore, these coefficients are subject to restrictive relations which follow from the symmetry of the crystal structure.[1] For example, they must all vanish for those crystals which possess a center of inversion.

In the linear electro-optic effect, $E_j^0E_k^\omega$ is physically distinguishable from $E_k^0E_j^\omega$ so that experiments are not

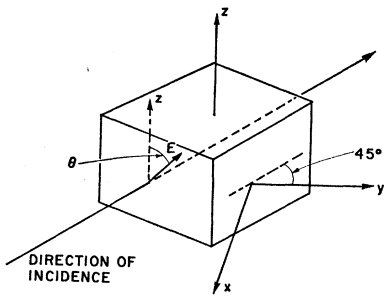

FIG. 1. The cut of crystal used in the present work. The z axis is placed normal to the capacitor plates, and dimensions in all cases were of the order of 1 cm. The angle θ is the angle between the optical electric field and the crystal's z axis.

* This research was supported in part by the U. S. Atomic Energy Commission and is based on a dissertation submitted by one of us (M.B.) in partial fulfillment of the requirements for the degree of Ph.D. in Physics at The University of Michigan.
† Present address: University of California, Berkely, California.
‡ Present address: Clarendon Laboratory, Oxford, England.
[1] For a general review of nonlinear optical phenomena with notation similar to that of the present paper, see P. A. Franken and J. F. Ward, Rev. Mod. Phys. **35**, 23 (1963).
[2] J. A. Armstrong, N. Bloembergen, J. Ducuing, and P. S. Pershan, Phys. Rev. **127**, 1918 (1962).

restricted to the determination of pairs of coefficients. However, arguments are readily developed[1] which demonstrate that $X_{jik}^{\omega}=X_{kij}^{\omega}$, irrespective of crystal-symmetry considerations, so that the number of *independent* parameters needed to describe optical rectification and the linear electro-optic effect in a given crystal are the same. Equations which relate the two effects are reviewed in Sec. III, together with the restrictions imposed by crystal symmetry on the tensor coefficients.

Optical rectification was first observed[3] in crystals of KH_2PO_4, KD_2PO_4, and later[4,5] in ZnTe, CdS, and $Cd(S_{0.75}+Se_{0.25})$. Measurements of the effect in quartz have also been reported.[6] In the present paper we describe the experiments on optical rectification in KH_2PO_4, KD_2PO_4, CdS, ZnTe, and $Cd(S_{0.75}+Se_{0.25})$. These results are compared with predictions based on the linear electro-optic effect. In addition, predictions of the relative values are developed from optical and dc dielectric data.

II. EXPERIMENTAL

The experiments described in this paper have in common the deployment of equipment to measure the

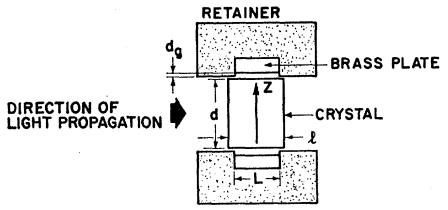

FIG. 2. A sectional view of the crystal-capacitor mounting. Dimensions are referred to in the Appendix, and the construction is discussed in the text.

voltage developed across various crystals during the passage of an intense beam of laser radiation. In each case, crystals of approximately one-centimeter dimensions were cut in the configuration of Fig. 1. The angle θ between the plane of polarization of the laser beam and the crystal z axis could be varied by rotating the laser. The crystals were mounted between brass plates as shown in Fig. 2, an arrangement which constitutes a parallel-plate capacitor with the crystal as a dielectric medium. The small voltages (typically a few hundred microvolts) developed between these plates were amplified and displayed with conventional techniques described briefly below, and in greater detail in Ref. 5.

It is important to prevent laser radiation from striking the brass plates because the attendant local-heating and photoionization phenomena lead to the development of spurious signals. In order to obviate these

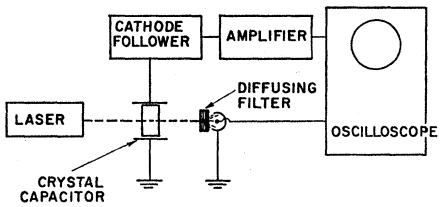

FIG. 3. A schematic diagram of the experiment.

effects, the retainers shown in Fig. 2 were fabricated from black bakelite, and each crystal was mounted so that the surfaces were separated from the brass plates by approximately 0.002 in. In addition, the crystals were highly polished to minimize the possibility of radiation being scattered directly onto the metal surfaces.

The voltage measurements were accomplished with the equipment illustrated in Fig. 3, and described in detail in Ref. 5. The over-all bandwidth of this system was 30 Mc/sec, determined largely by the dual-beam oscilloscope response, and was sufficient to follow the approximately 30-nsec rise and decay times of the laser pulses. The intensity and time dependence of the laser radiation was monitored with a photocell sheltered behind a diffusing filter, as indicated in Fig. 3. The time constant of the cathode follower input circuit was *large* compared with the duration of the laser pulse, in order to insure that the development and decay of voltages across the metal plates of the capacitor were determined by the induced polarization of the crystal rather than circuit parameters.

The ruby laser was a commercial[7] unit which provided pulses of approximately 1-MW intensity with a full width of about 100 nsec. For the studies at 10 600 Å, a giant-pulse neodymium-doped glass laser was constructed as described in Ref. 5. This equipment provided pulses of up to 5 MW, with full widths of about 100 nsec.

The elements of the optical-rectification tensor are restricted by the crystal symmetry as shown in Table I for the crystals of present interest. These restrictions played an important role in determining our choice of geometry for the experiments. There are, however, two further considerations. Firstly, the electrodes of the crystal capacitor must be kept out of the laser beam to avoid the development of spurious signals. This makes it most convenient to measure only those components of the polarization which are perpendicular to the light-propagation direction. Secondly, it is essential to select situations where the two electric-field components have the same phase velocity in the crystal. This is analogous to the index-matching problem encountered in second-harmonic generation.[1]

Data for the experiments described in this section and the formulas necessary for their reduction to the optical-rectification coefficients are given in the Appen-

[3] M. Bass, P. A. Franken, J. F. Ward, and G. Weinreich, Phys. Rev. Letters **9**, 446 (1962).
[4] M. Bass, Bull. Am. Phys. Soc. **8**, 624 (1963).
[5] M. Bass, Ph.D. thesis, University of Michigan, 1964 (unpublished).
[6] M. Subramanian, Ph.D. thesis, Purdue University, 1964 (unpublished).
[7] LSI-Laser Systems Center Model LS-2 with rotating mirror attachment.

TABLE I. The nonvanishing coefficients X_{ijk}^0 of the optical-rectification tensor. Table (a) is for crystals of class V_d (KH_2PO_4 and KD_2PO_4). For class T_d crystals (ZnTe), (a) is appropriate when all the constants are set equal. (b) is for class C_{6v} [CdS and $Cd(S_{0.75}+Se_{0.25})$].

		jk / i	x x	y y	z z	y z	z x	x y	z y	x z	y x
(a)	X_{ijk}^0	x	0	0	0	a	0	0	b	0	0
		y	0	0	0	0	b	0	0	a	0
		z	0	0	0	0	0	c	0	0	c

		jk / i	x x	y y	z z	y z	z x	x y	z y	x z	y x
(b)	X_{ijk}^0	x	0	0	0	0	h	0	0	g	0
		y	0	0	0	g	0	0	h	0	0
		z	d	d	f	0	0	0	0	0	0

dix. Reflection, scattering and absorption of the laser beam by the crystal and the details of the cathode follower input circuit are considered in that analysis. Our values for the optical-rectification coefficients are summarized in Table II.

1. Absolute Measurement of Optical Rectification in KH_2PO_4

Our absolute determination of optical rectification in KH_2PO_4 has been described elsewhere[3,5] and yielded the value $(X_{zxy}^0+X_{zyx}^0)=5\times10^{-8}$ esu, with an estimated uncertainty of a factor of 3. In this section we will review details of this experiment that are appropriate to the work of the present paper.

Figure 4(a) reproduces a photograph of a dual-beam oscilloscope trace in which the upper beam displays the intensity of the laser light and the lower beam displays the voltage detected across the KH_2PO_4 crystal. For this trace, the angle θ was 90°. Figure 4(b) was obtained under the same circumstances but with the angle θ set at 0°, in which case the optical rectification signal is expected to vanish [see Appendix, Eq. (A13)]. Attention is called to the change in baseline which occurs at the time of the pulse. We believe this is due to a residual pyroelectric effect because it is independent of the angle θ and decays slowly. The delay between the upper and lower traces is due to a 3×10^{-8}-sec delay in the amplifier system.

The $\sin^2\theta$ dependence of the optical rectification signal (see Appendix) was verified in these experiments[3] in order to strengthen the identification of the optical-rectification effect. This data is shown in Fig. 5.

The primary contribution to the error quotation of a factor 3 is the uncertainty of a factor 2 in the calibration of the laser-beam power. In order to achieve this calibration, the filter and photocell of Fig. 3 were standardized against a commercial calorimeter.[8] The remaining contributions to our estimated uncertainty arise primarily from the measurements of various circuit parameters and scatter in the measured signal-voltage–to–power ratios.

TABLE II. The optical-rectification coefficients measured at 6943 Å, together with predictions made from the linear electro-optic data of R. O'B. Carpenter [J. Opt. Soc. Am. **25**, 1145 (1953)]. The relative values are considered reliable to within 50%, while the absolute determinations are uncertain to within a factor 3.

Crystal	Coefficient	Relative	Absolute $\times10^{-8}$ esu	Prediction $\times10^{-8}$ esu
KH_2PO_4	$(X_{zxy}^0+X_{zyx}^0)$	1	5	6.0
KD_2PO_4	$(X_{zxy}^0+X_{zyx}^0)$	2.1	10.5	12.9
CdS	$X_{zxx}^0=X_{zyy}^0$	9	45	···
CdS	X_{zzz}^0	7	35	···
$Cd(S_{0.75}+Se_{0.25})$	$X_{zxx}^0=X_{zyy}^0$	29	145	···
ZnTe	$(X_{zxy}^0+X_{zyx}^0)$	73	365	···

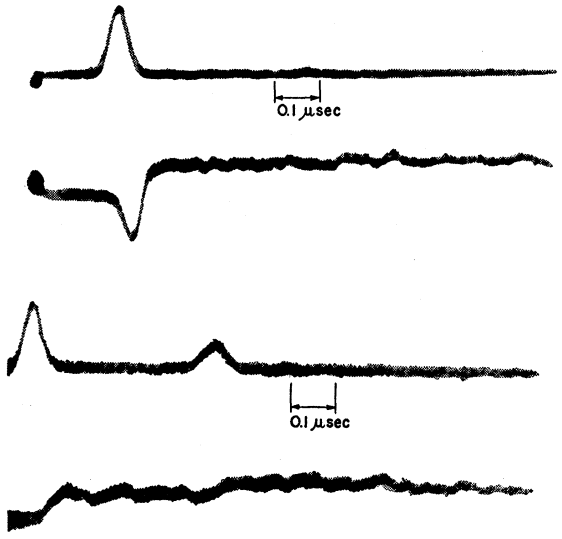

FIG. 4. Photographs of a dual-beam oscilloscope trace in which the upper beam shows the intensity of the laser light and the lower shows the signal from a KH_2PO_4 crystal, time increasing toward the right. In Fig. 4(a) the angle θ was 90°, and the amplitude of the signal from the crystal was 200 μV. In Fig. 4(b) the angle θ was 0°. (This figure is reproduced from Ref. 3.)

2. Relative Measurements

The measurement of optical rectification coefficients in various crystals *relative* to KH_2PO_4 was undertaken because of the greater accuracy attainable when explicit measurement of the laser power is avoided.

The deuterated salt, KD_2PO_4, was investigated by making alternate measurements with this crystal and a standard KH_2PO_4 crystal in the arrangement of Fig. 3.

A different technique was used for the three crystals CdS, $Cd(S_{0.75}+Se_{0.25})$ and ZnTe. A new crystal capacitor, with separate cathode follower, was located in the position of the photocell shown in Fig. 3. Each crystal, in turn, was then placed into this unit so that the laser beam first passed through the KH_2PO_4 and

[8] LSI-Laser Systems Center calorimeter MI-2.

then through the crystal under investigation. The ratio of the signals determines the ratio of the optical rectification coefficients.

For CdS the signal is present at both $\theta=0$ and 90° but arises from different elements of the optical-rectification tensor. The ratio of those elements was determined in experiments with the arrangement shown in Fig. 3.

The results of these relative measurements are displayed in Table II and are believed to be accurate to within 50%

3. Experiments with Neodymium Laser

An absolute measurement of the optical-rectification coefficient of ZnTe at 10 600 Å was accomplished by using the neodymium laser in an arrangement similar to that of Fig. 3. However, for this experiment, the optical power was measured with a transmission device[9] placed between the laser and the crystal. We

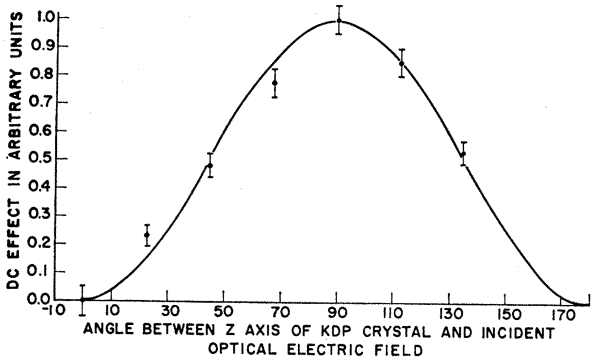

FIG. 5. The variation with angle θ of the measured ratio of the optical-rectification signal in KH_2PO_4 to the laser intensity, normalized at $\theta=90°$. The solid curve is the function $\sin^2\theta$, and the data are taken from Ref. 3.

find $(X_{zxy}^0+X_{zyx}^0)=104\times10^{-8}$ esu. This determination is considered reliable to within a factor 3, with error considerations virtually identical to those given in Sec. II.1 for the work with ruby lasers.

We had intended to measure optical rectification in ZnTe relative to KH_2PO_4 at the neodymium wavelength (10 600 Å) in order to explore the wavelength sensitivity discussed in Sec. IV. This study was frustrated by a curious interfering signal that appears in the observation of optical rectification in KH_2PO_4 under excitation at the neodymium wavelength. In Fig. 6(a) is shown a photograph of the dual-beam oscilloscope display in which the upper beam exhibits the neodymium laser intensity and the lower shows the signal developed across the KH_2PO_4 sample. This figure is to be compared with Fig. 4(a) for the same arrangement using ruby radiation. The shift in baseline is so striking

[9] This was the same type of calorimeter used in the KH_2PO_4 determination but, unfortunately, was a different model with an independent calibration.

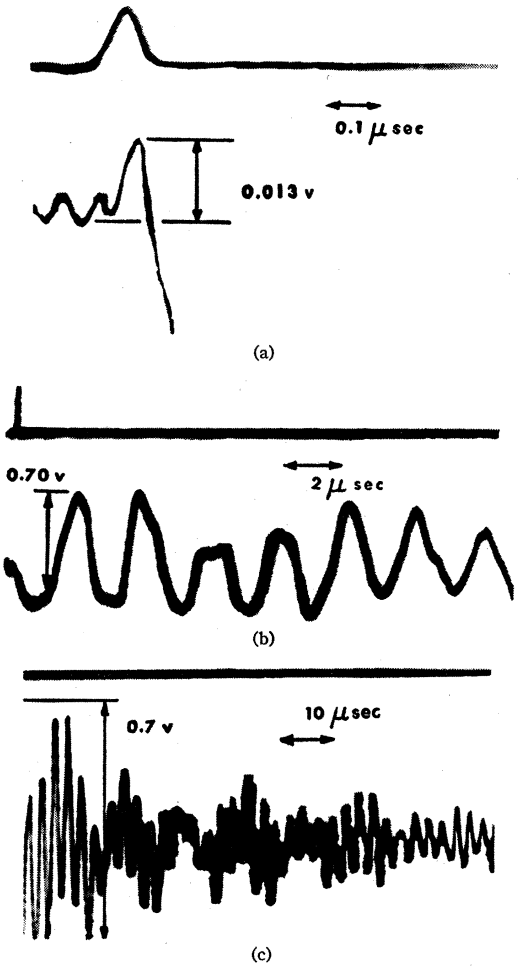

FIG. 6. Photographs of a dual-beam oscilloscope trace in which the upper beam shows the neodymium-laser light intensity and the lower shows the signal from a KH_2PO_4 sample. The angle $\theta=90°$ in each.

as to preclude a meaningful determination of the optical rectification signal. Figures 6(b) and 6(c) were achieved with the same experimental conditions but much slower sweepspeeds. The evidence of a large "ringing" effect is very striking, and in distinct contrast to the work with ruby radiation where the effect was insignificant.

We believe this interfering signal is due to a piezoelectric voltage which accompanies a mechanical oscillation in the crystal, and which is excited by a slight absorption of the neodymium-laser pulse. Despite the good transparency of KH_2PO_4 at 10 600 Å, there appears to be enough absorption from the infrared band to stimulate a mechanical oscillation in the crystal sufficient to account for the interfering signal. A detailed discussion of this effect is presented in Ref. 5.

4. Temperature Dependence of Optical Rectification in KH_2PO_4 and KD_2PO_4

The temperature dependence of optical rectification in KH_2PO_4 and KD_2PO_4 was initially studied by placing

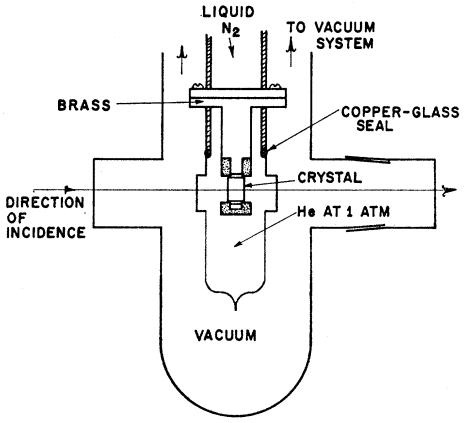

FIG. 7. Cryostat used in the temperature dependence measurements.

the crystal capacitor of Fig. 2 in an evacuated enclosure, with means for chilling the crystal and its mount to liquid-nitrogen temperature. Testing of this equipment revealed that large, spurious signals were developed which we believe arose from ions and electrons ejected by the laser beam from the crystal surfaces. The vacuum environment permitted these particles to create electrical havoc with the input stage of the cathode follower. Accordingly, a chamber was designed so that the crystals and mount could be enclosed in an atmosphere of helium and still be cooled. The helium, at atmospheric pressure, served a dual purpose. It prevented the development of the spurious signals and it also helped to provide uniform cooling of the crystal. Figure 7 shows the essential features of this system. The various plane surfaces were situated and painted in such a way as to minimize the possibility of laser radiation being scattered to the plates of the capacitor. The crystal temperature was monitored with a copper-constantan thermocouple attached to that plate of the capacitor which was electrically grounded.

Our measurements of the temperature dependence of the optical rectification effect in KH_2PO_4 and KD_2PO_4 are shown in Fig. 8, together with additional data on the electro-optic effect which is taken from the work of Zwicker and Scherrer.[10] Both sets of data are normalized to unity at 300°K. The accuracy of the optical-rectification measurements is about 20% at room temperature, and deteriorates to a factor of 2 at the low-temperature end owing to uncertainty in the large correction for the gap capacitance. These corrections (see Appendix) become very large at low temperatures in these crystals owing to the increase in dielectric constant as the ferroelectric transition temperature is approached.

III. THEORY

In this section the theory of optical rectification and the linear electro-optic effect is reviewed for subsequent comparison with the experimental results.

[10] B. Zwicker and P. Scherrer, Helv. Phys. Acta **17**, 346 (1944).

A quantum-mechanical treatment of the tensors $\mathbf{X}$ defined by Eqs. (I.1) involves matrix elements and frequencies characteristic of the crystal and, although these are largely unknown, the approach does form a useful basis for discussion. The problem was first treated in this way by Armstrong *et al.*[2] and subsequently discussed elsewhere.[1,11] The results taken from Ref. 11 are:

$$\begin{aligned}(X_{ijk}^{0}+X_{ikj}^{0})=(e^3/2\hbar^2)S^0\textstyle\sum_{nn'}\{&[\langle r_j\rangle_{ng}\langle r_k\rangle_{n'g}\langle r_i\rangle_{nn'}\\&+\langle r_k\rangle_{ng}\langle r_j\rangle_{n'g}\langle r_i\rangle_{nn'}]C_{nn'}\\&+[\langle r_i\rangle_{ng}\langle r_j\rangle_{n'g}\langle r_k\rangle_{nn'}+\langle r_i\rangle_{ng}\langle r_k\rangle_{n'g}\langle r_j\rangle_{nn'}]D_{nn'}\\&+[\langle r_j\rangle_{ng}\langle r_i\rangle_{n'g}\langle r_k\rangle_{nn'}+\langle r_k\rangle_{ng}\langle r_i\rangle_{n'g}\langle r_j\rangle_{nn'}]D'_{nn'}\},\end{aligned} \tag{III.1}$$

$$\begin{aligned}X_{jik}^{\omega}=(e^3/\hbar^2)S^\omega\textstyle\sum_{nn'}\{&[\langle r_j\rangle_{ng}\langle r_k\rangle_{n'g}\langle r_i\rangle_{nn'}\\&+\langle r_k\rangle_{ng}\langle r_j\rangle_{n'g}\langle r_i\rangle_{nn'}]C_{nn'}\\&+[\langle r_i\rangle_{ng}\langle r_k\rangle_{n'g}\langle r_j\rangle_{nn'}+\langle r_i\rangle_{ng}\langle r_j\rangle_{n'g}\langle r_k\rangle_{nn'}]D_{nn'}\\&+[\langle r_j\rangle_{ng}\langle r_i\rangle_{n'g}\langle r_k\rangle_{nn'}+\langle r_k\rangle_{ng}\langle r_i\rangle_{n'g}\langle r_j\rangle_{nn'}]D'_{nn'}\},\end{aligned} \tag{III.2}$$

where, for example, $\langle r_i\rangle_{nn'}$ is the matrix element of x, y, or z between the states n and n', which are excited states. The ground state is denoted by g. S^0 and S^ω are included to relate microscopic and macroscopic field quantities and are discussed below. The frequency-dependent terms $C_{nn'}$, $D_{nn'}$, and $D'_{nn'}$ are

$$\begin{aligned}C_{nn'}&=\frac{1}{2}\left[\frac{1}{(\omega_{ng}+\omega)(\omega_{n'g}+\omega)}+\frac{1}{(\omega_{ng}-\omega)(\omega_{n'g}-\omega)}\right],\\D_{nn'}&=\frac{1}{2}\left[\frac{1}{\omega_{ng}(\omega_{n'g}+\omega)}+\frac{1}{\omega_{ng}(\omega_{n'g}-\omega)}\right],\\D'_{nn'}&=\frac{1}{2}\left[\frac{1}{(\omega_{ng}+\omega)\omega_{n'g}}+\frac{1}{(\omega_{ng}-\omega)\omega_{n'g}}\right],\end{aligned} \tag{III.3}$$

where, for example, ω_{ng} denotes the difference in energy between the states n and g in units of angular frequency, and ω is the angular frequency of the optical electric field.

S^0 and S^ω may be evaluated using the Lorentz factor to relate local and applied fields,[12] in which case

$$S=S^0=S^\omega=(\tfrac{1}{3}(\epsilon^\omega+2))^2(\tfrac{1}{3}(\epsilon^0+2))N, \tag{III.4}$$

where ϵ is the dielectric constant at frequencies indicated by superscripts and N is the number density of cells in the crystal. This analysis has two limitations. Firstly, it applies only to media with isotropic dielectric constants and, secondly, the local field so derived from the applied field is the *average* over the unit cell whereas it is the local field *at the site of the nonlinear interaction* which is required. The approximation is least good for crystals with large and very anisotropic dielectric con-

[11] J. F. Ward and P. A. Franken, Phys. Rev. **133**, A183 (1964).
[12] H. A. Lorentz, *Theory of Electrons* (B. G. Teubner, Leipzig, 1909), pp. 138, 306.

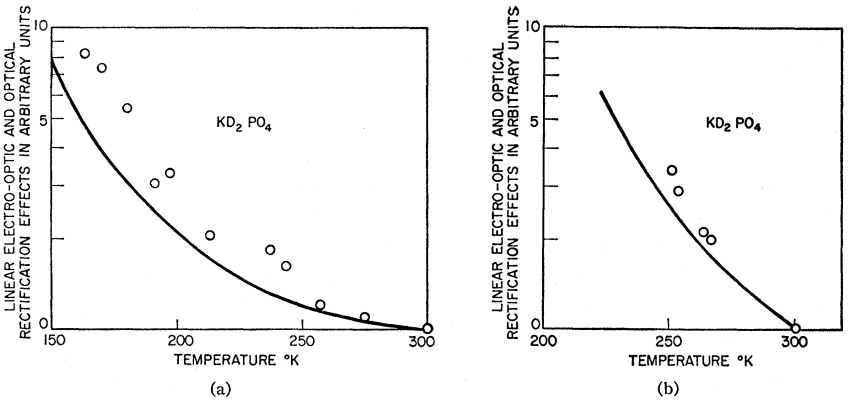

FIG. 8. A comparison of the temperature dependence of the optical-rectification effect (open circles) with that of the linear-electro-optic effect (solid curves) for KH_2PO_4 and KD_2PO_4. The linear-electro-optic data are taken from Ref. 10, and both sets of data are normalized to 300°K.

stants, but it still provides a useful basis for the discussion of experimental results.

An important quantitative relationship between optical rectification and the linear electro-optic effect is found from inspection of Eqs. (III.1) and (III.2):

$$(X_{ijk}{}^0+X_{ikj}{}^0)=\tfrac{1}{2}X_{jik}{}^\omega=\tfrac{1}{4}(X_{jik}{}^\omega+X_{kij}{}^\omega). \quad \text{(III.5)}$$

This equation permits the prediction of optical-rectification coefficients in a given crystal from measurements of the linear electro-optic effect. However, the experimental data for the linear electro-optic effect are usually tabulated in terms of tensor elements r_{jki} which relate explicitly to the modification of optical indices of refraction in the presence of a dc electric field. We now derive the relationship between these two tensors.

The equation which defines the tensor elements r_{jki} is

$$\epsilon_{jk}{}'^{-1}=\epsilon_{jk}{}^{-1}+r_{jki}E_i{}^0, \quad \text{(III.6)}$$

where $\epsilon_{jk}{}'^{-1}$ is the jk element of the *inverse* optical dielectric tensor $\epsilon_{jk}{}^{-1}$, as it is modified in the presence of the dc electric field $E_i{}^0$. By definition, the modified dielectric tensor elements $\epsilon_{jk}{}'$ are given by

$$\epsilon_{jk}{}'=\epsilon_{jk}+4\pi p_j{}^\omega/E_k{}^\omega. \quad \text{(III.7)}$$

The $p_j{}^\omega$ are specified in terms of the electric fields and the tensor elements $X_{jik}{}^\omega$ by Eq. (I.1b) so that Eq. (III.7) may be rewritten

$$\epsilon_{jk}{}'=\epsilon_{jk}+4\pi X_{jik}{}^\omega E_i{}^0. \quad \text{(III.8)}$$

It is now convenient to specify a coordinate system in which the dielectric tensor is diagonal. Noting that $\boldsymbol{\epsilon}'^{-1}\cdot\boldsymbol{\epsilon}'\equiv\mathbf{1}$, Eqs. (III.6) and (III.8) can be combined [neglecting terms in $(E_i{}^0)^2$] to yield

$$r_{jki}=-(4\pi/\epsilon_{kk}\epsilon_{jj})X_{jik}{}^\omega. \quad \text{(III.9)}$$

The ϵ_{ii} are the squares of the principal indices of refraction so that for the present case of uniaxial crystals $\epsilon_{xx}=\epsilon_{yy}=n_0{}^2$ and $\epsilon_{zz}=n_e{}^2$, where n_0 and n_e are the ordinary and extraordinary indices of refraction, respectively.

The third-rank tensor components of interest in this paper are all symmetric under interchange of the two subscripts referring to fields or polarization of the same frequency[13]:

$$\tfrac{1}{2}(X_{ijk}{}^0+X_{ikj}{}^0)=\tfrac{1}{2}(X_{ikj}{}^0+X_{ijk}{}^0), \quad \text{(III.10a)}$$

$$X_{jik}{}^\omega=X_{kij}{}^\omega, \quad \text{(III.10b)}$$

$$r_{jki}=r_{kji}. \quad \text{(III.10c)}$$

These symmetric subscripts j and k are sometimes contracted to a single index m running from 1 to 6 according to the combinations xx, yy, zz, yz, zx, xy.

It is customary to contract r according to

$$r_{jki}=r_{kji}\equiv r_{mi}. \quad \text{(III.11)}$$

X^0 and also the second-harmonic tensor $X^{2\omega}$ may be similarly contracted, but at least two conventions appear in the literature:

$$(X_{ijk}+X_{ikj})=(2-\delta_{jk})X_{im}$$
or
$$(X_{ijk}+X_{ikj})=2X_{im}. \quad \text{(III.12)}$$

We avoid ambiguity in the present paper by adhering to the full three-index notation.

IV. COMPARISON OF EXPERIMENT WITH THEORY

1. Relationship between Optical Rectification and the Linear Electro-Optic Effect

Our experimental results for the optical rectification coefficients are listed in Table II, together with values predicted from available linear electro-optic coefficients using Eqs. (III.5) and (III.9). The agreement is well within the factor of 3 error in the absolute experimental coefficients. For KH_2PO_4 and KD_2PO_4, the clamped electro-optic coefficients are used because the duration

[13] Equation (III.10a) is clearly an identity. However, the symmetry under interchange of j and k should not be used to infer that $X_{ijk}{}^0=X_{ikj}{}^0$ because, in general (that is, unless $k=j$) only the *pairs* of elements which appear in Eq. (III.10a) are meaningful or measurable. Equation (III.10b) follows from Eq. (III.2), or from a thermodynamic argument. Here a *single* element is measurable and therefore meaningful. Equation (III.10c) follows from Eqs. (III.10b) and (III.9).

of the laser pulse is short compared to the fundamental acoustical period of the crystals. The measurement for KD_2PO_4 of 2.1 ± 1.0, relative to KH_2PO_4, is in excellent agreement with the value of 2.15 predicted from the linear electro-optic data.

The temperature dependence of the optical rectification and linear electro-optic coefficients[10] is compared for both KH_2PO_4 and KD_2PO_4 in Figs. 8(a) and 8(b). The data are normalized at room temperature. Unfortunately, the very large correction for the gap capacitance that has to be taken to reduce the optical rectification data provides an uncertainty of a factor of 2 in the low-temperature regions. Thus, it is only possible to assert that the temperature dependences of optical rectification and the linear electro-optic effect are very similar, consistent with the theoretical expectation that they are identical. It is interesting to note that KD_2PO_4 has a ferroelectric transition at about 208°K, below which point the crystal symmetry precludes the observation of an optical-rectification signal with the present geometry. This prediction was confirmed experimentally, which serves as a further check on the nature of our signals.

The striking temperature dependence of optical rectification and the linear electro-optic effect in KH_2PO_4 is in marked contrast to the observation[14] that second-harmonic generation in this crystal is virtually independent of temperature down to the Curie point. We believe that this can be accounted for by considerations of the role played by the dc dielectric constant, which enters into the evaluation of the optical rectification coefficients [Eq. (III.4)].

2. Prediction of the Nonlinear Coefficients from Linear Data

The optical-rectification coefficients listed in Table II have values extending over nearly two orders of magnitude. The motivation for the investigation of CdS, $Cd(S_{0.75}+Se_{0.25})$, and ZnTe arose from the proximity of their band edges to the laser frequency. It was expected that this situation would enhance the coefficients. The observed effects in these crystals are indeed found to be larger than in KH_2PO_4, and it is now of interest to predict the relative values of the coefficients from somewhat more detailed but necessarily schematic arguments based on the available linear dielectric data.

Equations (III.1), (III.3), and (III.4) provide an explicit expression for the optical-rectification coefficients, within the limitations discussed in connection with the Lorentz factor derivation of Eq. (III.4). We now seek to evaluate the required matrix elements and characteristic frequencies from refractive index data.

The linear optical dielectric tensor elements ϵ_{ij}^{ω} are given by

$$\frac{(\epsilon_{ij}^{\omega}-1)}{(\epsilon_{ij}^{\omega}+2)}=\frac{4\pi}{3}\frac{e^2}{\hbar}\sum_n \langle r_i\rangle_{gn}\langle r_j\rangle_{ng} \times\left[\frac{1}{\omega_{ng}-\omega}+\frac{1}{\omega_{ng}+\omega}\right]\cdot N, \quad \text{(IV.1)}$$

where N is the number density of the relevant atomic systems. A convenient simplification is achieved by going to a scalar form (ignoring the birefringence of the crystals) and also replacing the matrix elements by an *effective* matrix element $\langle r\rangle_{ng}$ and the frequencies ω_{ng} by an *effective* characteristic frequency ω_0. Omitting the uninteresting constants, Eq. (IV.1) reduces to an equation of the Clausius-Mossotti form:

$$\frac{n^2-1}{n^2+1}\propto N\langle r\rangle_{ng}^2\left[\frac{1}{\omega_0-\omega}+\frac{1}{\omega_0+\omega}\right]. \quad \text{(IV.2)}$$

The refractive-index data[15] as a function of frequency are fitted to Eq. (IV.2) and yield values for $N\langle r\rangle_{ng}^2$ and ω_0 as listed in Table III.

Similar simplification of the nonlinear expressions [Eqs. (III.1) and (III.4)] leads to a relationship of the form

$$\mathbf{X}^0\propto N(n^2+2)^2(\epsilon^0+2)\langle r\rangle_{gn}\langle r\rangle_{nn'}\langle r\rangle_{n'g}[C+D+D']. \quad \text{(IV.3)}$$

The frequency factor $(C+D+D')$ appearing here may be evaluated from Eq. (III.3) with $\omega_{n'g}$ and ω_{ng} set equal to an *effective* characteristic frequency ω_0' for the nonlinear process. This implies that we are restricting discussion to the case where both the excited levels which dominate optical rectification are in the optical absorption band (an electronic-electronic process). This has been found to be a reasonable conjecture for the analysis of nonlinear phenomena in KH_2PO_4.[11]

We can now evaluate relative values of $\mathbf{X}^0$ from Eq. (IV.3). The factor $(n^2+2)^2(\epsilon^0+2)$ follows directly from data in the literature[15] and the factor $N\langle r\rangle_{ng}^2$ from the linear data is used for $N\langle r\rangle_{gn}\langle r\rangle_{n'g}$. In the absence of data on which to base an estimate for $\langle r\rangle_{nn'}$ we assume that it is the same for all crystals. It remains only to estimate a value for the nonlinear effective characteristic frequency ω_0'. The nonlinear process gives more weight to levels near the laser frequency than does the linear process, due to the quadratic frequency denominators in C, D, and D', so that a correct estimate for ω_0' should lie between ω_0 and the band edge at ω_b. Table III shows the estimates for $\mathbf{X}^0$ relative to KH_2PO_4, which result from various choices of ω_0', together with the experimental data for $\mathbf{X}^0$. The

[14] J. P. van der Ziel and N. Bloembergen, Phys. Rev. **135**, A1662 (1964).

[15] The refractive data for KH_2PO_4 are taken from The International Critical Tables and we are grateful to J. M. Jost and L. R. Shiozawa for private communication of data for CdS, CdSe, and ZnTe.

TABLE III. Predictions of relative values of the optical-rectification coefficients in various crystals. ω_b is the band edge, and ω_0 is the effective characteristic frequency for the optical index of refraction [Eq. (IV.2)]. The columns a, b, c, and d refer to values of the quantity $2(C+D+D')$ evaluated for ω_0' set equal to ω_0, $\frac{1}{2}(\omega_0+\omega_b)$, $(\omega_0\omega_b)^{1/2}$, or ω_b, respectively [see Eq. (III.3) and Sec. IV.2]. The quantities $N\langle r\rangle_{n0}^2$ and $(n^2+2)^2(\epsilon^0+2)$ are evaluated as described in Sec. IV.2. The predictions a′, b′, c′, and d′ are the normalized products of the two previous columns and one of the columns a, b, c, and d, respectively. The last column lists the experimental results displayed in Table II, but with the values for CdS and $Cd(S_{0.75}+Se_{0.25})$ doubled in order that all the entries refer to a pair of coefficients.

			$2(C+D+D')$ $(\text{eV})^{-2}$						Predictions				
			a	b	c	d							
Crystal	ω_b (eV)	ω_0 (eV)	Band center	Arithmetic mean	Geometric mean	Band edge	$N\langle r\rangle_{n0}^2$	$(n^2+2)^2(\epsilon^0+2)$	a′	b′	c′	d′	Experiment
KH_2PO_4	6.9	14.2	0.0317	0.0511	0.0639	0.142	1.00	415	1	1	1	1	1
KD_2PO_4	6.9	14.2	0.0317	0.0511	0.0639	0.142	1.00	940	2.3	2.3	2.3	2.3	2.1
CdS	2.42	6.6	0.157	0.315	0.548	5.81	0.91	782	8.5	11	15	70	18
$Cd(S_{0.75}+Se_{0.25})$	2.09	6.3	0.171	0.480	0.748	14.6	0.88	782	9.0	16	19	171	58
ZnTe	2.23	10.7	0.0550	0.168	0.319	7.49	1.84	1460	11	21	32	342	73

experimental values for CdS and $Cd(S_{0.75}+Se_{0.25})$ from Table II have been doubled so that the values in Table III all refer to a *pair* of coefficients.

It can be seen from Table III that the predictions agree with the experimental values to within a factor 7 for any estimate of ω_0' in the range ω_0 to ω_b and to within a factor 4 for the reasonable assignments $\omega_0'=(\omega_0\omega_b)^{1/2}$ or $\frac{1}{2}(\omega_0+\omega_b)$. Since the experimental data for the various crystals range over a factor 70, we feel that these theoretical estimates have some validity and interest.

Prediction of the dispersion of X^0 for ZnTe between the ruby and neodymium wavelengths is on a firmer basis because we can assume that the matrix elements and local field factors S^0 are unchanged. However, the experimental ratio of the coefficients at these two wavelengths is uncertain to within a factor 3, thus precluding a meaningful comparison of prediction with experiment for this case.

ACKNOWLEDGMENTS

It is a pleasure to acknowledge our fruitful conversations with Robert C. Miller and Gabriel Weinreich.

APPENDIX

In this Appendix we describe the calculations necessary for determining the optical rectification coefficients $\mathbf{X}^0$ from the experimental data.

The amplitude E^ω of the optical electric field at a point in a medium is related to the power P of a traveling wave by

$$(E^\omega)^2=8\pi P/ncA\,, \tag{A1}$$

where n is the optical-refractive index of the crystal, c is the velocity of light in free space and A is the cross-sectional area of the beam. In the present experiments there are losses and reflections, so that we require a value for the optical field averaged over the effective length of the crystal, in terms of either the power P_0 incident on the crystal, or the power P_t transmitted by the crystal:

$$\begin{aligned}(E^\omega)^2&=8\pi P_0G_0/ncA\\&=8\pi P_tG_t/ncA\,.\end{aligned} \tag{A2}$$

In these equations G_0 and G_t are functions of the surface reflection coefficient R, the surface scattering coefficient S (which will be arbitrarily taken as 0.03 for all the crystals), and the bulk attenuation coefficient per unit length α:

$$\begin{aligned}G_t=(1/\alpha l')\{&(e^{-(\frac{1}{2}\alpha)(l-l')}-e^{-(\frac{1}{2}\alpha)(l+l')})\\&+\mathrm{Re}^{-2\alpha l}(e^{(\frac{1}{2}\alpha)(l+l')}-e^{(\frac{1}{2}\alpha)(l-l')})\}\\&\times(e^{+\alpha l}/(1-R-S))\end{aligned} \tag{A3}$$

$$\begin{aligned}G_0=(1/\alpha l')\{&(e^{-(\frac{1}{2}\alpha)(l-l')}-e^{-(\frac{1}{2}\alpha)(l+l')})\\&+\mathrm{Re}^{-2\alpha l}(e^{(\frac{1}{2}\alpha)(l+l')}-e^{(\frac{1}{2}\alpha)(l-l')})\}(1-R-S)\,.\end{aligned} \tag{A4}$$

The lengths L, l, and l' are measured in the propagation direction of the light beam (see Fig. 2). L is the capacitor plate length (0.6 cm for the all experiments), l is the crystal length and l' is that length of crystal which is effective in developing the optical-rectification signal. For those cases where $l\leq L$, we take $l'=l$. However, for those crystals which were longer than the capacitor plates (CdS, ZnTe, KD_2PO_4) an average value of the quantity lG_0 or lG_t is used for the final data reduction:

$$\begin{aligned}\langle lG_0\rangle_{\mathrm{av}}&=\tfrac{1}{2}[l'G_0(l'=l)+l'G_0(l'=L)]\,,\\\langle lG_t\rangle_{\mathrm{av}}&=\tfrac{1}{2}[l'G_t(l'=l)+l'G_t(l'=L)]\,.\end{aligned} \tag{A5}$$

The geometry of these experiments is such that the laser beam is incident in the x-y plane at 45° to the x and y axes. (The coordinate system is that of the crystal.) The angle between the optical electric field and the z axis is θ, so that

$$\begin{aligned}E_x^\omega=E_y^\omega&=(E_0^\omega\sin\theta)/\sqrt{2}\,,\\E_z^\omega&=E_0^\omega\cos\theta\,.\end{aligned} \tag{A6}$$

The dc polarization $\mathbf{p}^0$ is related to the field amplitudes by Eq. (I.1a). p_z^0 is the only component of interest when the capacitor plates are in the xy plane and the coefficients X_{ijk}^0 are subject to the symmetry restriction appropriate to each crystal (see Table I). For KH_2PO_4

TABLE IV. Experimental crystal parameters. R is the surface reflection coefficient, α is the bulk attenuation coefficient per unit length measured at 6943 Å, n is the index of refraction, and ϵ is the appropriate dc dielectric constant. The dimensions l, d and d_g are shown in Fig. 2. The quantity $(1+\epsilon d_g/d)$ is computed from the data of the table, and the final computed averages $\langle G_0 l\rangle_{\rm av}$ (cm) and $\langle G_t l\rangle_{\rm av}$ (cm) are listed in the last two columns. [See Eqs. (A2) through (A5).]

Crystal	Class	R	α (cm^{-1})	n	ϵ	l (cm)	d (cm)	d_g (cm)	$1+\epsilon d_g/d$	$\langle G_0 l\rangle_{\rm av}$ (cm)	$\langle G_t l\rangle_{\rm av}$ (cm)
KH_2PO_4-I	V_d	0.04	0	1.5	21	0.5	1.35	0.01	1.16		0.56
KH_2PO_4-II	V_d	0.04	0	1.5	21	0.5	0.6	0.02	1.7		0.56
KD_2PO_4	V_d	0.04	0	1.5	50	0.8	0.55	0.01	1.9		0.79
CdS	C_{6v}	0.18	0.529	2.5	9.5	0.85	0.9	0.01	1.11	0.53	
$Cd(S_{0.75}+Se_{0.25})$	C_{6v}	0.18	3.76	2.5	9.5	0.5	0.4	0.01	1.24	0.19	
ZnTe	T_d	0.25	1.57	3.0	10.1	0.8	0.9	0.01	1.11	0.30	

and KD_2PO_4 (crystal class V_d) and for ZnTe (crystal class T_d),

$$p_z^0=(X_{zxy}^0+X_{zyx}^0)E_x^\omega E_y^\omega$$
$$=\tfrac{1}{2}(X_{zxy}^0+X_{zyx}^0)\sin^2\theta E_0^2, \quad \text{(A7)}$$

and for CdS and $Cd(S_{0.75}+Se_{0.25})$ (crystal class C_{6v})

$$p_z^0=X_{zxx}^0(E_x^\omega)^2+X_{zyy}^0(E_y^\omega)^2+X_{zzz}^0(E_z^\omega)^2$$
$$=\tfrac{1}{2}(X_{zxx}^0+X_{zyy}^0)\sin^2\theta+X_{zzz}^0\cos^2\theta(E_0^\omega)^2, \quad \text{(A8)}$$

where in this case, symmetry considerations require that $X_{zxx}^0=X_{zyy}^0$.

The crystal capacitors may be treated as sections of infinite plane parallel capacitors to a good approximation because the crystals of the present experiments all have large dc dielectric constants. In this approximation it may be shown[5] that the voltage V induced across the capacitor is proportional to the induced dipole moment and independent of its distribution throughout the crystal:

$$V=p_z^0Al'/dC, \quad \text{(A9)}$$

where l' is the effective length discussed above, d is the distance between the capacitor plates, C is the capacitance of the crystal capacitor, and A is the cross-sectional area of the beam.

The experimental situation is complicated by the presence of additional capacitors: the two crystal-plate airgaps, with total capacitance C_g and the cathode follower input capacitance. The total capacitance C_t is measured across the cathode follower input with the crystal capacitor connected. The cathode follower responds to the potential V' developed at its input, which differs from V, the voltage which would be developed across the isolated crystal. V' is given by

$$V'=\frac{p_z^0Al'}{dC_t(1+C/C_g)}. \quad \text{(A10)}$$

It is convenient to express C/C_g in terms of the crystal dielectric constant ϵ, its height d and the gap thickness d_g, so that Eq. (A10) can be written

$$V'=\frac{p_z^0Al'}{dC_t(1+\epsilon d_g/d)}. \quad \text{(A11)}$$

In the experiments at room temperature, the largest value of the factor $(1+\epsilon d_g/d)$ is 1.9 for the case of KD_2PO_4 and the smallest is 1.11 for the case of ZnTe and CdS.

The compilation of Eqs. (A2), (A6), (A7), (A8), and (A11) yields the expressions required for computing the optical-rectification coefficients from the experimental data:

$$\frac{V'C_t(1+\epsilon d_g/d)cnd}{8\pi\langle Gl\rangle_{\rm av}P}=\tfrac{1}{2}(X_{zxy}^0+X_{zyx}^0)\sin^2\theta$$
for V_d and T_d crystals
$$=\tfrac{1}{2}(X_{zxx}^0+X_{zyy}^0)\sin^2\theta+X_{zzz}^0\cos^2\theta$$
for C_{6v} crystals. (A12)

In these equations, $\langle Gl\rangle_{\rm av}P$ denotes either $\langle G_t l\rangle_{\rm av}P_t$ or $\langle G_0 l\rangle_{\rm av}P_0$, depending on whether transmitted or incident laser power is measured.

Table IV lists the parameters of each crystal, and Table V gives the experimental data used for the determination of the optical-rectification coefficients displayed in Table II of the text.

TABLE V. The experimental data used for the determination of the optical-rectification coefficients displayed in Table II of the text. C_T is the total circuit capacitance, and θ is the angle defined in Fig. 1. The column V'/P lists the measured ratios of the signal and the laser power in each experiment. The units are millivolts per megawatt, or are relative, as indicated adjacent to each entry. The data shown in the last row were taken with the neodymium laser; all of the other experiments were performed with ruby radiation.

Crystal	C_T(pf)	θ	V'/P
KH_2PO_4-I	9.0	90°	1.9 mV/MW
KH_2PO_4-I	9.0	90°	1
KD_2PO_4	9.5	90°	4.2 } relative
KH_2PO_4-II	14.0	90°	1
CdS	12.0	90°	12.3 } relative
KH_2PO_4-II	14.0	90°	1
$Cd(S_{0.75}+Se_{0.25})$	14.9	90°	22.8 } relative
KH_2PO_4-II	11.8	90°	1
ZnTe	35.4	90°	6.68 } relative
CdS	12.0	90°	1
CdS	12.0	0°	0.76 } relative
ZnTe	21.0	90°	9.4 mV/MW